

A cascade model of ventricular-arterial coupling and arterial-cardiac baroreflex  
function for cardiovascular variability in humans

Shigeki Shibata, Rong Zhang, Jeff Hastings, Qi Fu,  
Kazunobu Okazaki, Ken-ichi Iwasaki, Benjamin D. Levine

From the Institute for Exercise and Environmental Medicine, Presbyterian Hospital of Dallas,  
and the University of Texas Southwestern Medical center at Dallas, Texas

Running Head: Dynamic ventricular-arterial coupling in humans

Correspondence to: Benjamin D. Levine, MD  
Institute for Exercise and Environmental Medicine  
7232 Greenville Ave, Suite 435, Dallas, TX 75231.  
Telephone: (214)345-4619  
Fax: (214)345-4618  
E-mail: BenjaminLevine@TexasHealth.org

## Abstract

*Background:* Cardiovascular variability reflects autonomic regulation of blood pressure (BP) and heart rate (HR). However, systolic BP (SBP) variability also may be induced by fluctuations in stroke volume through left ventricular end diastolic pressure (LVEDP) variability via dynamic ventricular-arterial coupling during respiration. We hypothesized that dynamic ventricular-arterial coupling is modulated by changes in left ventricular compliance associated with altered preload and that a cascade control mechanism of ventricular-arterial coupling with arterial-cardiac baroreflex function contributes to the genesis of cardiovascular variability at the respiratory frequency.

*Methods and Results:* Seven healthy young subjects underwent six minute recordings of beat-by-beat LVEDP, SBP and HR in the supine position with controlled respiration at 0.2 Hz during hyper- and hypovolemia. Spectral and transfer function analysis of these variables was conducted between 0.18-0.22 Hz. Dynamic ventricular-arterial coupling gain (Gain LVEDP-SBP) was smaller by 25% ( $P=0.009$ ) during hypervolemia than hypovolemia while arterial-cardiac baroreflex function gain (Gain SBP-HR) was similar. As predicted from a cascade model, a linear relationship between Gain LVEDP-HR and LVEDP-SBP times Gain SBP-HR was identified ( $R^2=0.93$ ,  $P<0.001$ ). Gain LVEDP-HR was smaller

by 40% ( $P=0.04$ ) during hypervolemia than hypovolemia, leading to a reduction in spectral power of HR variability by 45% ( $P=0.08$ ).

*Conclusion:* We conclude that dynamic ventricular-arterial coupling gain is reduced during hypervolemia due to a decrease in left ventricular compliance. A cascade model of ventricular-arterial coupling with the arterial-cardiac baroreflex contributes to the genesis of cardiovascular variability at the respiratory frequency.

Key words: Heart rate variability, Blood pressure variability, Cardiac mechanics

## Introduction

Quantification of cardiovascular variability has been established as a tool to examine autonomic function in patients with cardiovascular disease (40). For example, patients with congestive heart failure (4, 34, 39) or with myocardial infarction (24, 44) show significantly depressed heart rate (HR) variability associated with increases in mortality. These observations have been attributed to the presence of impaired autonomic function interacting with the presence of cardiovascular disease. However, since HR variability is only the output variable of complicated cardiovascular and respiratory control systems, both neural and non-neural control mechanisms may contribute to the changes in HR variability (12, 37, 46, 48).

Short-term HR variability at respiratory frequencies is likely to be produced by the complicated interactions between the arterial-cardiac baroreflex (3, 31, 37) and central respiratory control mechanisms (13). Although the specific mechanisms underlying short-term HR variability are still under debate (3, 13, 31, 37), it is generally accepted that HR variability at the respiratory frequency is modulated by efferent vagal activity to the sinus node, because it is largely eliminated by atropine (12, 37).

Conversely, recent studies have demonstrated significant contributions of non-neural control mechanisms for BP variability at the respiratory frequency

because BP variability at the respiratory frequency did not change after complete autonomic blockade (37, 48). In addition, several studies demonstrated the existence of stroke volume (SV) variability at the respiratory frequency (14, 16, 21, 42), suggesting that SV variability may lead to BP variability via non-neural ventricular-arterial coupling. Specifically, we have speculated that changes in cardiac filling volume during respiration produce changes in left ventricular end diastolic pressure (LVEDP) via the left ventricular pressure-volume relationship (Fig. 1) (2, 26). Sequentially, changes in LVEDP (preload) produce changes in SV, and hence SBP (afterload) via the Starling mechanism (Fig. 1) (2, 26). Of note, both of these relationships also are affected by changes in intrathoracic pressure per se during respiration via ventricular interdependence and/or transmural pressure changes (16, 21). Therefore, it is conceivable that the dynamic transmission properties between the LVEDP and SBP (dynamic ventricular-arterial coupling) are likely to be determined by the specific slopes of the cardiac mechanical curves as illustrated in Fig 1.

It is generally accepted that the baroreflex transfers SBP variability into changes in HR via the modulation of autonomic neural activity (47). Since SBP variability at the respiratory frequency is produced primarily by the non-neural control of dynamic ventricular-arterial coupling (14, 16, 21, 37, 42, 48), HR variability at the respiratory frequency would be produced at least partly by the

cascade mechanism of dynamic ventricular-arterial coupling with the arterial-cardiac baroreflex (Fig. 1).

The primary aim of the present study was to test the hypothesis that dynamic ventricular-arterial coupling is modulated by changes in left ventricular compliance associated with changes in left ventricular preload. Furthermore, we hypothesized that a cascade control mechanism of ventricular-arterial coupling with arterial-cardiac baroreflex function contributes to the genesis of cardiovascular variability at the respiratory frequency.

For these aims, we used a two-component cascade model to determine both the individual and the combined effects of dynamic ventricular-arterial coupling and the arterial-cardiac baroreflex for the genesis of SBP and HR variability under hypo- and hypervolemic conditions. Hypovolemia was induced after administration of a diuretic agent (furosemide) and hypervolemia with normal saline infusion. The purpose of these interventions was to alter the operating points of dynamic ventricular-arterial coupling located on the cardiac mechanical curves as indicated in Fig 1 in order to test the specific hypothesis of this study.

## **Methods**

### *Subjects*

Seven sedentary nonsmoking healthy men (ages 20 to 35) with a BMI of  $25 \pm 0.6 \text{ kg/m}^2$  participated in this study. All subjects were screened with a detailed medical history, a physical examination, and a baseline 12-lead ECG. The study was performed in accordance with the Declaration of Helsinki. The experimental procedures were explained to all subjects with informed consent obtained as approved by the Institutional Review Boards of the University of Texas Southwestern Medical Center at Dallas and Presbyterian Hospital.

### *Measurements*

For each subject, the RR interval was continuously monitored using a 3-lead ECG (Hewlett-Packard). Photoplethysmography (Finapres, Ohmeda) was used to continuously measure finger arterial blood pressure (ABP) with the transducer positioned at heart level. For measurements of pulmonary capillary wedge pressure (PCWP) and pulmonary arterial pressure (PAP) a 6-F balloon-tipped, fluid filled catheter (Swan-Ganz, Baxter) was placed through an antecubital vein into the pulmonary artery under fluoroscopic guidance. All intracardiac pressures were referenced to atmospheric pressure, with the pressure transducer (Transpac IV, Abbott) zero reading set at 5 cm below the sternal angle. The mean PCWP was determined visually at end expiration. Beat-by-beat pulmonary artery diastolic pressure (PAD) was used as an index of beat-by-beat LVEDP to avoid prolonged

balloon inflation for safety reasons (15). Cardiac output was measured with a modified acetylene rebreathing technique using acetylene as the soluble and helium as the insoluble gas (27, 43). Then cardiac output and heart rate during the rebreathing were used to calculate the SV. Baseline plasma volume (PV) was measured by Evans blue dye and then changes in PV were estimated during hypervolemia and hypovolemia from hematocrit changes according to the method of Van Beaumont (45).

### *Experimental protocol*

All experiments were performed in the morning at least 2h after a light breakfast in a quiet environmentally controlled laboratory with an ambient temperature of 25°C. The subjects were asked to refrain from heavy exercise and caffeinated or alcoholic beverages for at least 24h before the tests. To assess the effect of central volume changes, two specific conditions of hypervolemia and hypovolemia were utilized. Subjects rested for at least 30 min in the supine position to stabilize their hemodynamics. Hypervolemia was then induced with warm (37°C) isotonic saline infusion of 30 ml/kg at a rate of 100-150 ml/min using an 18 gauge intravenous catheter and an infusion bag pressurized to 250 mmHg. Our previous studies showed that this amount and rate of saline infusion leads clearly to higher left ventricular end diastolic volume, SV and PCWP (2, 26).

Pulmonary arterial pressure was monitored continuously and PCWP was measured intermittently during saline infusion for safety reasons. Immediately after saline infusion, SV and PCWP were measured and then subjects were asked to breathe at a controlled 12/min frequency for six minutes by following a moving cursor on a breathing pattern displayed on a computer. The breathing pattern used was an equal amplitude and equal time interval of saw-tooth waveforms. All subjects followed the breathing protocol very well without complaint of any discomfort. We selected a controlled frequency breathing to avoid changes in HR variability induced by changes in respiratory patterns during spontaneous breathing (6, 18) and to avoid changes in BP variability at the respiratory frequencies being contaminated by those fluctuations at the lower frequencies ( $<0.15$  Hz) (30). Six-minute data segments of PAP, ABP and ECG were recorded for spectral and transfer function analysis. Hypovolemia was induced on a separate occasion with intravenous administration of 20 mg of furosemide (Lasix). After administration of furosemide, the change in PCWP was monitored continuously over 2 hours to confirm an approximately 25% reduction of PCWP (33). The same measurements for spectral and transfer function analysis as during hypervolemia were performed under hypovolemic conditions. These two experiments were separated by at least 3 days but no more than 3 weeks. In addition, a 6 min random frequency breathing protocol with an averaged frequency of  $15 \pm 11$ /min was performed before the

controlled breathing protocol during both hypervolemia and hypovolemia to confirm our assumption that beat-by-beat changes in LVEDP are induced mainly by respiration and that changes in SBP and HR variability during changes in central volume have little if any effect on the changes in LVEDP.

### *Data analysis*

#### *Spectral and transfer function estimation*

PAP, ABP and ECG waveforms were sampled at 1 kHz and digitized at 12 bits with an A/D converter (Das-20, Metrabyte). Digitized signals were stored in a laboratory computer and processed with a custom-designed program for PAD, SBP and R wave detection. Beat-to-beat LVEDP (estimated from PAD), SBP and HR (calculated from R-R interval) were linearly interpolated and then resampled at 2 Hz for spectral analysis. The time series of LVEDP, SBP and HR were first detrended with third-order polynomial fitting and then subdivided into 256 point segments with 50% overlap for spectral estimation. This process resulted in five segments of data over the 6 min period recordings. Fast Fourier transforms were implemented with each Hanning-windowed data segment and then averaged to calculate auto-spectra  $[S_{X,X}(f)]$  and cross-spectra  $[S_{X,Y}(f)]$  for LVEDP, SBP and HR variability respectively. The spectral resolution for these estimates is 0.0078 Hz.

To quantify the dynamic relationship between SBP and HR variability, transfer function analysis between these variables was used (20, 25, 31, 37). Similarly, transfer function between changes in preload (LVEDP) and afterload (SBP) of the left ventricle was estimated to quantify dynamic ventricular-arterial coupling (49). Therefore, transfer function  $[H(f)]$  of dynamic ventricular-arterial coupling  $[H_{L-S}(f)]$ , arterial-cardiac baroreflex function  $[H_{S-H}(f)]$  and the total transfer function  $[H_{L-H}(f)]$  between the LVEDP and HR variability were obtained with the following equations:

$$H_{L-S}(f) = S_{LVEDP-SBP}(f)/S_{LVEDP-LVEDP}(f) \quad (1)$$

$$H_{S-H}(f) = S_{SBP-HR}(f)/S_{SBP-SBP}(f) \quad (2)$$

$$H_{L-H}(f) = S_{LVEDP-HR}(f)/S_{LVEDP-LVEDP}(f) \quad (3)$$

Where  $S_{LVEDP-SBP}(f)$ ,  $S_{SBP-HR}(f)$ , and  $S_{LVEDP-HR}(f)$  are cross spectra between LVEDP and SBP, SBP and HR, and LVEDP and HR, respectively.  $S_{LVEDP-LVEDP}(f)$  and  $S_{SBP-SBP}(f)$  are the auto-spectra of LVEDP and SBP, respectively. Transfer function gain and phase were derived from the real part  $[H_R(f)]$  and the imaginary part  $[H_I(f)]$  of the complex transfer function as

$$|\text{Gain}(f)| = \{[H_R(f)]^2 + [H_I(f)]^2\}^{1/2} \quad (4)$$

$$\text{Phase}(f) = \tan^{-1}[H_I(f)/H_R(f)] \quad (5)$$

Gain and phase reflect the relative amplitude and time relationships between the input and output signals of the system modeled by  $H(f)$  over a specified frequency range.

Coherence function was derived from  $S_{X.X}(f)$ ,  $S_{Y.Y}(f)$  and  $S_{X.Y}(f)$  as

$$\text{Coherence} = |S_{X.Y}(f)|^2 / [S_{X.X}(f) S_{Y.Y}(f)] \quad (6)$$

The reliability of linear transfer function estimation was evaluated by the estimates of coherence function in this study.

Since coherence function between LVEDP and SBP variability was low ( $< 0.5$ ) at the frequency range below 0.15 Hz even when random breathing was applied (Fig.2, Fig.4), we used data at the high frequency range between 0.18 and 0.22 Hz during controlled frequency breathing (0.2 Hz) to estimate transfer functions between LVEDP, SBP and HR variability, where coherence function was high ( $>0.5$ ) under all experimental conditions.

The spectral power of LVEDP, SBP and HR also was calculated in the high frequency range (0.18-0.22 Hz) by integrating the corresponding auto-spectra (20, 37, 48). Mean values of gain, phase and coherence were calculated in the high frequency range and averaged for all subjects under hypo- and hypervolemic conditions (20, 37, 48).

Finally to validate the proposed two-component cascade model, the relationship between the product of Gain LVEDP-SBP and Gain SBP-HR, and the estimation

of Gain LVEDP-HR was assessed by using linear regression of all the data obtained under hypo- and hypervolemic conditions (23, 38).

### *Statistics*

Variables were compared between hypovolemia and hypervolemia by paired t-test. A p value of  $< 0.05$  was considered statistically significant. Data are presented as means  $\pm$  SE.

## **Results**

### *Steady-state Hemodynamics*

PCWP, PAD, SV and PV all were significantly higher during hypervolemia than hypovolemia (Table 1), consistent with the expected increases in central volume. HR and SBP were significantly higher during hypervolemia than hypovolemia (Table 1). Total HR and SBP variability quantified by standard deviation of the time series were significantly lower during hypervolemia (Table 1).

### *Spectral and transfer function analysis*

Representative data of time series and autospectra in LVEDP, SBP, and HR during control breathing from one subject are shown in Fig. 2. Averaged data of autospectra in LVEDP, SBP, and HR in hyper- and hypovolemia during control breathing are shown in Fig. 2. Averaged data of transfer function and coherence function in hyper- and hypovolemia during control breathing are shown in Fig. 3. Averaged data of autospectra in LVEDP, SBP and HR, and coherence function during random breathing are shown in Fig. 4.

High frequency power of LVEDP was significantly higher during hypervolemia than hypovolemia (Table 1) (Fig. 5) ( $P < 0.05$ ). High frequency power of HR variability tended to decrease during hypervolemia, but did not reach statistical significance (Table 1) ( $P = 0.08$ ). High frequency power of SBP variability was not changed (Table 1).

Peak values of coherence ( $> 0.8$ ) were observed around the respiratory frequency for all transfer functions (LVEDP-HR, LVEDP-SBP, and SBP-HR) (Fig. 3). The mean values of coherence function were above 0.5 for all transfer functions in the high frequency range, indicating the reliability of transfer function gain and phase estimates in the high frequency range.

Gain LVEDP-SBP was significantly lower during hypervolemia than hypovolemia (Fig. 3, Fig. 5, Fig. 7) (hypovolemia;  $1.31 \pm 0.09$ , hypervolemia;  $0.97 \pm 0.12$  mmHg/mmHg,  $P = 0.009$ ). However, no change in Gain SBP-HR was

observed between hypovolemia and hypervolemia (Fig. 3, Fig. 7) (hypovolemia;  $1.31 \pm 0.19$ , hypervolemia;  $1.18 \pm 0.22$  beat/min/mmHg,  $P=0.19$ ). Gain LVEDP-HR was significantly lower during hypervolemia than hypovolemia (Fig. 3, Fig. 7) (hypovolemia;  $2.09 \pm 0.56$ , hypervolemia;  $1.25 \pm 0.28$  beat/min/mmHg,  $P=0.04$ ).

As expected, a strong linear relationship ( $R^2=0.93$ ,  $P<0.001$ ) was observed between the product of Gain LVEDP-SBP and Gain SBP-HR and the estimate of Gain LVEDP-HR (Fig. 6).

Phase of LVEDP-SBP was significantly lower in hypervolemia than hypovolemia (Fig. 3) (hypovolemia;  $-0.24 \pm 0.23$ , hypervolemia;  $-0.68 \pm 0.20$  radian,  $P = 0.01$ ). Phase of LVEDP-SBP was negative in the high frequency ranges in 11 of 14 data sets (7 subjects tested during hyper- and hypovolemia). Phase of SBP-HR and LVEDP-HR were positive in all data and were not different between hypervolemia and hypovolemia (Fig. 3).

## Discussion

We obtained three major results that provide new evidence for the presence of non-neural control mechanisms for the genesis of cardiovascular variability in humans. First, we found that dynamic ventricular-arterial coupling gain (Gain LVEDP-SBP) was reduced significantly during hypervolemia as compared to hypovolemia. These data suggest that a reduction in dynamic left ventricular

compliance due to hypervolemia results in smaller changes in SV per unit changes in LVEDP, and hence smaller changes in SBP under dynamic conditions (Fig. 5). Second, the presence of a strong linear relationship between the product of Gain LVEDP-SBP and Gain SBP-HR and the estimation of Gain LVEDP-HR demonstrates the validity of using a cascade model of cardiac mechanics with arterial-cardiac baroreflex function to identify the non-neural control mechanisms of cardiovascular variability in humans (23, 38) (Fig. 6, Fig. 7). Finally, these findings suggest that left ventricular diastolic function may affect HR variability at the respiratory frequency via dynamic ventricular-arterial coupling rather than exclusively due to autonomic mechanism (Fig. 1, Fig. 7).

### *Steady-state Hemodynamics*

As expected by protocol and confirmed from PV changes, both PCWP and SV increased during hypervolemia, suggesting an upward shift of the operating point on both the left ventricular pressure-volume and the Starling curves (Fig. 1). The increase in steady state SBP during hypervolemia was likely caused by an increase in SV and cardiac output. HR was higher in hypervolemia than hypovolemia, consistent with the presence of a Bainbridge reflex during hypervolemia (17, 32).

### *Dynamic ventricular-arterial coupling*

We assessed the transmission properties of preload (LVEDP) to afterload (SBP) of the left ventricle by using the cross spectral method. In previous studies (2, 26), we have shown that the operational slope on the Starling curve, which determines the dynamic transmission properties between the beat-by-beat change in LVEDP and SV, decreased during hypervolemia. Consistent with these observations, a significant decrease in dynamic ventricular-arterial coupling gain (Gain LVEDP-SBP) was observed during hypervolemia in the present study (Fig. 5).

As we expected, prominent power of LVEDP variability and the highest coherence function between LVEDP and SBP were observed at the controlled respiratory frequency of 0.2 Hz (Fig. 2, Fig. 3). Moreover, LVEDP power at frequencies lower than 0.15 Hz was much larger during random than fixed frequency breathing (Fig. 2, Fig. 4). These findings support our assumption that LVEDP changes are caused primarily by respiration, and that LVEDP changes produce SV and thus SBP variability via the pressure-volume and Starling mechanisms. Our results showed that the phase relationship of LVEDP-SBP was negative for most subjects under either hypo- or hypervolemic conditions, suggesting that changes in LVEDP precede SBP. These findings also are consistent with our assumption that changes in LVEDP produce changes in SBP via ventricular-arterial coupling. Furthermore, it is also possible that a dilated right

ventricular chamber during hypervolemia alters the operational slopes of the pressure-volume and Starling curves via ventricular interdependence (16, 21). In addition, changes in intrathoracic pressure during respiration per se also may alter the operational slopes of cardiac mechanical curves by changing transmural pressure (16, 21). However, regardless of the specific underlying mechanisms, the results of the present study support the hypothesis that dynamic ventricular-arterial coupling is dependent on cardiac preload due to changes in operational slopes on the cardiac mechanical curves that lead to the changes in SBP variability at respiratory frequencies.

High frequency power of LVEDP increased in hypervolemia as compared to hypovolemia. These changes may be explained by the pressure-volume relationship of left ventricle. For example, if changes in cardiac filling volume due to respiration were equal between the hypervolemia and hypovolemia, the pressure changes would be larger during hypervolemia than hypovolemia because of the upward shifting of the operating point to a less compliant portion on the pressure-volume curve (Fig. 5). This finding implies that the input variable of dynamic ventricular-arterial coupling, i.e., LVEDP variability, is also affected by left ventricular preload conditions.

*The reliability of cascade model*

LVEDP spectral power at frequency range  $< 0.15$  Hz in fixed frequency breathing was much less than that during random frequency breathing while similar SBP and HR spectral powers were observed between these conditions (Fig. 2, Fig. 4). These findings suggest, but do not necessarily prove that “feed-back” effects of SBP and HR variability on LVEDP variability, if any, are negligible under the current experimental conditions, supporting the “open- loop” cascade model hypothesis of this study. Furthermore, the presence of a strong linear relationship ( $R^2=0.93$ ,  $P<0.001$ ) between the estimate of Gain LVEDP-HR and the product of Gain LVEDP-SBP and Gain SBP-HR suggests the feasibility of using the proposed cascade model to represent both non-neural and neural control of cardiovascular variability at respiratory frequencies in humans (23, 38).

In the high frequency range, mean values of coherence function were above 0.5 for all transfer function estimates. These data support the statistical reliability of transfer function gain estimation in this study.

High frequency power of HR variability tended to decrease during hypervolemia. We attribute these changes at least partially to the reductions in the transfer function gain of LVEDP-SBP as suggested by the cascade model (Fig 1, Fig. 7). In addition, HR variability also could be influenced directly by changes in respiration (6, 18). Since carefully controlled frequency breathing was used to avoid the effect of changes in respiratory patterns on HR variability, the direct

effects of respiration on changes in HR variability are likely to be small between the experimental conditions in the present study (6, 18). We also cannot exclude mechanisms other than the cascade model to explain the reduction in HR variability at respiratory frequency during hypervolemia. For example, changes in LVEDP may affect autonomic nervous system activity and hence HR variability via cardiopulmonary receptors (13). Furthermore, at least theoretically the Bainbridge reflex could directly contribute to changes in Gain LVEDP-HR and hence HR variability, although the exact mechanism and neural pathways underlying this reflex in humans is uncertain (32).

### *Clinical implications*

It is possible that the effects of diastolic dysfunction on dynamic ventricular-arterial coupling and hence HR variability are more prominent in patients with congestive heart failure (CHF) and/or coronary artery disease rather than that caused by an experimentally increased preload condition in healthy young volunteers. Several studies support this assumption. For example, studies in CHF patients showed either a linear (1) or a logarithmic (7) relationship between the ejection fraction of left ventricle and the high frequency power of HR variability. Also, a positive relationship between high frequency power of heart rate variability and ejection fraction or mean acceleration of aortic flow was present in patients

with coronary artery disease (5). Moreover, patients with restrictive cardiac diastolic filling showed a greater reduction in heart rate variability (35).

The fact that continuous positive airway pressure (CPAP) improves prognosis in CHF patients, has been explained by a reduction of sympathetic activity (19, 22) and hence ventricular arrhythmias (36), associated with a reduction of cardiac work caused by changes in ventricular interdependence and/or reduction in transmural pressure due to intrathoracic positive pressure (29, 41). Our present findings suggest that CPAP also may improve dynamic ventricular-arterial coupling by changing the operational slopes on the pressure-volume and Starling curves via ventricular interdependence and/or changes in transmural pressure in CHF patients (29, 41). Therefore, it is possible that improvement in dynamic ventricular-arterial coupling per se is related to the treatment effects of CPAP on CHF patients.

### *Study Limitations*

There remains the possibility that HR changes affect SBP variability and hence Gain LVEDP-SBP through cardiac output changes since cardiac output is the product of HR and SV. It has been reported however that *systolic* blood pressure variability at the respiratory frequency is mainly determined by changes in SV which produces pulse pressure via arterial compliance, while *mean* blood pressure

variability is more closely related with cardiac output changes (9, 14, 28, 42). Theoretically, the transfer function gain between LVEDP and SBP variability could be decomposed into two components, i.e., a gain between LVEDP and SV variability via the Starling mechanism and a gain between SV and SBP variability via end-systolic ventricular-arterial coupling, reflecting arterial compliance (10). Therefore, our findings of changes in Gain LVEDP-SBP could reflect either ventricular or arterial compliance, although it is unlikely that arterial compliance would change significantly during our present study protocol. In order to evaluate dynamic ventricular-arterial coupling in more detail, future studies will be required to estimate beat-to-beat SV variability which will enable us to assess Gain LVEDP-SV and Gain SV-SBP separately.

Arterial-cardiac baroreflex function also may be affected by physiological changes other than volume status after saline infusion. For example, sodium sensitive arterial baroreflex sensors may change arterial-cardiac baroreflex function due to chronic sodium loading during large changes in sodium intake (11). Furthermore, changes in plasma osmolality may also affect baroreflex function after hypertonic saline infusion (8). In addition, HR variability may be affected by physiological mechanisms such as respiratory gating (13) or the Bainbridge reflex (32) in concert with arterial-cardiac baroreflex. Therefore, it is possible that arterial-cardiac baroreflex gain was similar between hypervolemia and

hypovolemia in the present study due to offsetting contributions of many physiological effects. However, whether *acute* changes in plasma sodium concentration affect the arterial baroreflex is uncertain, moreover the changes in plasma osmolality and sodium concentration are likely to be small after “isotonic” saline infusion. Therefore we speculate that the impact of these factors is likely to be small.

In conclusion, our results show that dynamic ventricular-arterial coupling gain (Gain LVEDP-SBP) was reduced significantly during hypervolemia as compared to hypovolemia probably due to a reduction in dynamic left ventricular compliance during hypervolemia. These changes may lead to a reduction in HR variability via a cascade model of dynamic ventricular-arterial coupling with arterial-cardiac baroreflex function. These findings suggest that a reduction of HR variability in patients with congestive heart failure may be at least partially explained by non-neural mechanisms of left ventricular diastolic dysfunction.

## References

1. **Ajiki K, Murakawa Y, Yanagisawa-Miwa A, Usui M, Yamashita T, Oikawa N, and Inoue H.** Autonomic nervous system activity in idiopathic dilated cardiomyopathy and in hypertrophic cardiomyopathy. *Am J Cardiol* 71: 1316-1320, 1993.
2. **Arbab-Zadeh A, Dijk E, Prasad A, Fu Q, Torres P, Zhang R, Thomas JD, Palmer D, and Levine BD.** Effect of aging and physical activity on left ventricular compliance. *Circulation* 110: 1799-1805, 2004.
3. **Baselli G, Cerutti S, Badilini F, Biancardi L, Porta A, Pagani M, Lombardi F, Rimoldi O, Furlan R, and Malliani A.** Model for the assessment of heart period and arterial pressure variability interactions and of respiration influences. *Med Biol Eng Comput* 32: 143-152, 1994.
4. **Bilchick KC, Fetics B, Djoukeng R, Fisher SG, Fletcher RD, Singh SN, Nevo E, and Berger RD.** Prognostic value of heart rate variability in chronic congestive heart failure (Veterans Affairs' Survival Trial of Antiarrhythmic Therapy in Congestive Heart Failure). *Am J Cardiol* 90: 24-28, 2002.
5. **Birand A, Kudaiberdieva GZ, Batyraliev TA, Akgul F, and Saliu S.** Relationship Between Components of Heart Rate Variability and Doppler Echocardiographic Indices of Left Ventricular Systolic Performance in Patients with Coronary Artery Disease. *International Journal of Angiology* 7: 244-248, 1998.
6. **Brown TE, Beightol LA, Koh J, and Eckberg DL.** Important influence of respiration on human R-R interval power spectra is largely ignored. *J Appl Physiol* 75: 2310-2317, 1993.
7. **Casolo GC, Stroder P, Sulla A, Chelucci A, Freni A, and Zeraushek M.** Heart rate variability and functional severity of congestive heart failure secondary to coronary artery disease. *Eur Heart J* 16: 360-367, 1995.
8. **Charkoudian N, Eisenach JH, Joyner MJ, Roberts SK, and Wick DE.** Interactions of plasma osmolality with arterial and central venous pressures in control of sympathetic activity and heart rate in humans. *Am J Physiol Heart Circ Physiol* 289: H2456-2460, 2005.
9. **Chemla D, Hebert JL, Coirault C, Zamani K, Suard I, Colin P, and Lecarpentier Y.** Total arterial compliance estimated by stroke volume-to-aortic pulse pressure ratio in humans. *Am J Physiol* 274: H500-505, 1998.
10. **Chen CH, Fetics B, Nevo E, Rochitte CE, Chiou KR, Ding PA, Kawaguchi M, and Kass DA.** Noninvasive single-beat determination of left ventricular end-systolic elastance in humans. *J Am Coll Cardiol* 38: 2028-2034, 2001.
11. **Creager MA, Roddy MA, Holland KM, Hirsch AT, and Dzau VJ.** Sodium depresses arterial baroreceptor reflex function in normotensive humans. *Hypertension* 17: 989-996, 1991.
12. **del Paso GA, Langewitz W, Robles H, and Perez N.** A between-subjects comparison of respiratory sinus arrhythmia and baroreceptor cardiac reflex sensitivity as non-invasive measures of tonic parasympathetic cardiac control. *Int J Psychophysiol* 22: 163-171, 1996.
13. **Eckberg DL.** The human respiratory gate. *J Physiol* 548: 339-352, 2003.
14. **Elstad M, Toska K, Chon KH, Raeder EA, and Cohen RJ.** Respiratory sinus arrhythmia: opposite effects on systolic and mean arterial pressure in supine humans. *J Physiol* 536: 251-259, 2001.
15. **Fisher ML, De Felice CE, and Parisi AF.** Assessing left ventricular filling pressure with flow-directed (Swan-Ganz) catheters. Detection of sudden changes in patients with left ventricular dysfunction. *Chest* 68: 542-547, 1975.

16. **Guz A, Innes JA, and Murphy K.** Respiratory modulation of left ventricular stroke volume in man measured using pulsed Doppler ultrasound. *J Physiol* 393: 499-512, 1987.
17. **Hakumaki MO.** Seventy years of the Bainbridge reflex. *Acta Physiol Scand* 130: 177-185, 1987.
18. **Hayano J, Mukai S, Sakakibara M, Okada A, Takata K, and Fujinami T.** Effects of respiratory interval on vagal modulation of heart rate. *Am J Physiol* 267: H33-40, 1994.
19. **Heindl S, Dodt C, Krahwinkel M, Hasenfuss G, and Andreas S.** Short term effect of continuous positive airway pressure on muscle sympathetic nerve activity in patients with chronic heart failure. *Heart* 85: 185-190, 2001.
20. **Iwasaki KI, Zhang R, Zuckerman JH, Pawelczyk JA, and Levine BD.** Effect of head-down-tilt bed rest and hypovolemia on dynamic regulation of heart rate and blood pressure. *Am J Physiol Regul Integr Comp Physiol* 279: R2189-2199, 2000.
21. **Karam M, Wise RA, Natarajan TK, Permutt S, and Wagner HN.** Mechanism of decreased left ventricular stroke volume during inspiration in man. *Circulation* 69: 866-873, 1984.
22. **Kaye DM, Mansfield D, Aggarwal A, Naughton MT, and Esler MD.** Acute effects of continuous positive airway pressure on cardiac sympathetic tone in congestive heart failure. *Circulation* 103: 2336-2338, 2001.
23. **Kreyszig E.** *Chapter 6 Laplace Transforms in Advanced Engineering Mathematics.* New York: John Wiley & Sons, 1993.
24. **La Rovere MT, Bigger JT, Jr., Marcus FI, Mortara A, and Schwartz PJ.** Baroreflex sensitivity and heart-rate variability in prediction of total cardiac mortality after myocardial infarction. ATRAMI (Autonomic Tone and Reflexes After Myocardial Infarction) Investigators. *Lancet* 351: 478-484, 1998.
25. **Laude D, Elghozi JL, Girard A, Bellard E, Bouhaddi M, Castiglioni P, Cerutti C, Cividjian A, Di Rienzo M, Fortrat JO, Janssen B, Karemaker JM, Leftheriotis G, Parati G, Persson PB, Porta A, Quintin L, Regnard J, Rudiger H, and Stauss HM.** Comparison of various techniques used to estimate spontaneous baroreflex sensitivity (the EuroBaVar study). *Am J Physiol Regul Integr Comp Physiol* 286: R226-231, 2004.
26. **Levine BD, Lane LD, Buckey JC, Friedman DB, and Blomqvist CG.** Left ventricular pressure-volume and Frank-Starling relations in endurance athletes. Implications for orthostatic tolerance and exercise performance. *Circulation* 84: 1016-1023, 1991.
27. **Levine BD, Zuckerman JH, and Pawelczyk JA.** Cardiac atrophy after bed-rest deconditioning: a nonneural mechanism for orthostatic intolerance. *Circulation* 96: 517-525, 1997.
28. **Lind L, Andren B, and Sundstrom J.** The stroke volume/pulse pressure ratio predicts coronary heart disease mortality in a population of elderly men. *J Hypertens* 22: 899-905, 2004.
29. **Naughton MT, Rahman MA, Hara K, Floras JS, and Bradley TD.** Effect of continuous positive airway pressure on intrathoracic and left ventricular transmural pressures in patients with congestive heart failure. *Circulation* 91: 1725-1731, 1995.
30. **Pagani M, Montano N, Porta A, Malliani A, Abboud FM, Birkett C, and Somers VK.** Relationship between spectral components of cardiovascular variabilities and direct measures of muscle sympathetic nerve activity in humans. *Circulation* 95: 1441-1448, 1997.
31. **Pagani M, Somers V, Furlan R, Dell'Orto S, Conway J, Baselli G, Cerutti S, Sleight P, and Malliani A.** Changes in autonomic regulation induced by physical training in mild hypertension. *Hypertension* 12: 600-610, 1988.

32. **Pawelczyk JA and Levine BD.** Cardiovascular Responses to Rapid Volume Infusion the Human Bainbridge Reflex. *Circulation* 92: 3148, 1995.
33. **Perhonen MA, Zuckerman JH, and Levine BD.** Deterioration of left ventricular chamber performance after bed rest: "cardiovascular deconditioning" or hypovolemia? *Circulation* 103: 1851-1857, 2001.
34. **Ponikowski P, Anker SD, Chua TP, Szelemej R, Piepoli M, Adamopoulos S, Webb-Peploe K, Harrington D, Banasiak W, Wrabec K, and Coats AJ.** Depressed heart rate variability as an independent predictor of death in chronic congestive heart failure secondary to ischemic or idiopathic dilated cardiomyopathy. *Am J Cardiol* 79: 1645-1650, 1997.
35. **Poulsen SH, Jensen SE, Moller JE, and Egstrup K.** Prognostic value of left ventricular diastolic function and association with heart rate variability after a first acute myocardial infarction. *Heart* 86: 376-380, 2001.
36. **Ryan CM, Usui K, Floras JS, and Bradley TD.** Effect of continuous positive airway pressure on ventricular ectopy in heart failure patients with obstructive sleep apnoea. *Thorax* 60: 781-785, 2005.
37. **Saul JP, Berger RD, Albrecht P, Stein SP, Chen MH, and Cohen RJ.** Transfer function analysis of the circulation: unique insights into cardiovascular regulation. *Am J Physiol* 261: H1231-1245, 1991.
38. **Sunagawa K, Sato T, and Kawada T.** Integrative sympathetic baroreflex regulation of arterial pressure. *Ann N Y Acad Sci* 940: 314-323, 2001.
39. **Szabo BM, van Veldhuisen DJ, van der Veer N, Brouwer J, De Graeff PA, and Crijns HJ.** Prognostic value of heart rate variability in chronic congestive heart failure secondary to idiopathic or ischemic dilated cardiomyopathy. *Am J Cardiol* 79: 978-980, 1997.
40. **Task.** Heart rate variability: standards of measurement, physiological interpretation and clinical use. *Circulation* 93: 1043-1065, 1996.
41. **Tkacova R, Rankin F, Fitzgerald FS, Floras JS, and Bradley TD.** Effects of continuous positive airway pressure on obstructive sleep apnea and left ventricular afterload in patients with heart failure. *Circulation* 98: 2269-2275, 1998.
42. **Toska K and Eriksen M.** Respiration-synchronous fluctuations in stroke volume, heart rate and arterial pressure in humans. *J Physiol* 472: 501-512, 1993.
43. **Triebwasser JH, Johnson RL, Burpo RP, Campbell JC, Reardon WC, and Blomqvist CG.** Noninvasive determination of cardiac output by a modified acetylene rebreathing procedure utilizing mass spectrometer measurements. *Aviat Space Environ Med* 48: 203-209, 1977.
44. **Tsuji H, Larson MG, Venditti FJ, Jr., Manders ES, Evans JC, Feldman CL, and Levy D.** Impact of reduced heart rate variability on risk for cardiac events. The Framingham Heart Study. *Circulation* 94: 2850-2855, 1996.
45. **Van Beaumont W.** Evaluation of hemoconcentration from hematocrit measurements. *J Appl Physiol* 32: 712-713, 1972.
46. **Wang YP, Cheng YJ, and Huang CL.** Spontaneous baroreflex measurement in the assessment of cardiac vagal control. *Clin Auton Res* 14: 189-193, 2004.
47. **Wray DW, Formes KJ, Weiss MS, AH OY, Raven PB, Zhang R, and Shi X.** Vagal cardiac function and arterial blood pressure stability. *Am J Physiol Heart Circ Physiol* 281: H1870-1880, 2001.

48. **Zhang R, Iwasaki K, Zuckerman JH, Behbehani K, Crandall CG, and Levine BD.** Mechanism of blood pressure and R-R variability: insights from ganglion blockade in humans. *J Physiol* 543: 337-348, 2002.
49. **Zhang R, Iwasaki K, Zuckerman JH, and Levine BD.** Ventricular-Arterial Coupling After Training Induced Left Ventricular Hypertrophy. *Circulation* 100: 730, 1999.

## Figure 1

The figure represents simple open loop model of the cascade of dynamic ventricular-arterial coupling and arterial-cardiac baroreflex function. G1 box represents dynamic ventricular-arterial coupling. Left and right panels in the G1 box represent pressure-volume curve and Starling curve of cardiac mechanics, respectively. The input signal of G1 is left ventricular end diastolic pressure (LVEDP) and the output signal is systolic blood pressure (SBP). Hypo and Hyper indicate the expected operating point during hypovolemia and hypervolemia, respectively. G2 represents arterial-cardiac baroreflex function. The input signal of G2 is SBP and the output signal is HR (R-R interval). G0 represents total transfer function consisted of series of G1 and G2. P and V, left ventricular end diastolic pressure and volume, respectively; SV, stroke volume; AP, arterial pressure.

## Figure 2

These figures represent time series (left panels) and autospectra (middle panels) of left ventricular end diastolic pressure (LVEDP) (estimated from pulmonary artery diastolic pressure), systolic blood pressure (SBP) and heart rate (HR) for a representative subject, and average of autospectra (right panels) of LVEDP, SBP and HR in hypervolemia and hypovolemia during controlled frequency breathing at 0.2 Hz.

### Figure 3

Transfer function coherence (left panels), gain (middle panels) and phase (right panels) of LVEDP to SBP (LVEDP-SBP), SBP to HR (SBP-HR), and LVEDP to HR (LVEDP-HR). Plots represent the mean transfer functions from all subjects. Hypervolemia (after acute saline infusion) and hypovolemia (after intra venous furosemide infusion) are displayed for each transfer function. Gray bars enhance high frequency range (0.18-0.22 Hz) in coherence function. LVEDP, left ventricular end diastolic pressure; SBP, systolic blood pressure; HR, heart rate.

### Figure 4

These figures represent average of autospectra (left panels) in left ventricular end diastolic pressure (LVEDP) (estimated from pulmonary artery diastolic pressure), systolic blood pressure (SBP) and heart rate (HR), and transfer function coherence (right panels) in LVEDP-SBP, SBP-HR and LVEDP-HR during random breathing. Gray bar enhances the frequency range where coherence function is higher than 0.5.

### Figure 5

Physiological explanation for the decrease in dynamic ventricular-arterial coupling gain (Gain LVEDP-SBP) and increase in high frequency power of left ventricular end diastolic pressure (HF LVEDP) during hypervolemia as compared to hypovolemia. \*:  $P < 0.05$ . SV, stroke volume; LVEDP and LVEDV, left ventricular end diastolic pressure and volume, respectively.

#### Figure 6

Gain of LVEDP to HR (Gain LVEDP-HR) plotted as a function of gain between LVEDP and SBP (Gain LVEDP-SBP) times gain between SBP and HR (Gain SBP-HR) for all data points of hypovolemia (after intra venous saline infusion) and hypervolemia (after acute saline infusion). The line represents linear regression for all data. LVEDP, left ventricular end diastolic pressure; SBP, systolic blood pressure; HR, heart rate.

#### Figure 7

Mean  $\pm$ SE for transfer function gain between LVEDP and HR (Gain LVEDP-HR), LVEDP and SBP (Gain LVEDP-SBP), and SBP and HR (Gain SBP-HR) calculated as the mean values of the curve of the transfer function gain at the high frequency (0.18-0.22 Hz). Hypervolemia (after acute saline infusion) is compared

with hypovolemia (after intravenous furosemide infusion). \*:  $P < 0.05$ . LVEDP, left ventricular end diastolic pressure; SBP, systolic blood pressure; HR, heart rate.

Table 1. Steady-state Hemodynamics and Spectral Analysis of LVEDP, SBP, and HR

	Hypovolemia	Hypervolemia
PV (ml)	3119±100	4398±158*
PCWP (mmHg)	7.4±1.0	16.8±1.6*
PAD (mmHg)	6.9±1.1	14.8±1.3*
PAD SD (mmHg)	1.5±0.2	1.8±0.2*
SV (ml)	86±7	105±8*
SBP (mmHg)	125±5	140±5*
SBP SD (mmHg)	6±1	5±0*
DBP (mmHg)	74±4	74±4
DBP SD (mmHg)	4±1	3±0*
HR (bpm)	69±3	80±3*
HR SD (bpm)	6±1	5±1*
HF LVEDP (mmHg <sup>2</sup> )	1.1±0.2	2.2±0.2*
HF SBP (mmHg <sup>2</sup> )	2.0±0.4	2.5±0.6
HF HR (bpm <sup>2</sup> )	5.6±2.3	3.1±0.9†

Values are means±SE. Hypovolemia, after intra venous furosemide injection; Hypervolemia, after acute saline infusion; SD, standard deviation of the time series; PV, Plasma volume; PCWP, pulmonary capillary wedge pressure; PAD, pulmonary artery diastolic pressure; SV, stroke volume; SBP and DBP, systolic and diastolic blood pressure, respectively; HR, heart rate; HF, spectral power in high frequency ranges (0.18-0.22 Hz); \* P < 0.05; † P = 0.08.

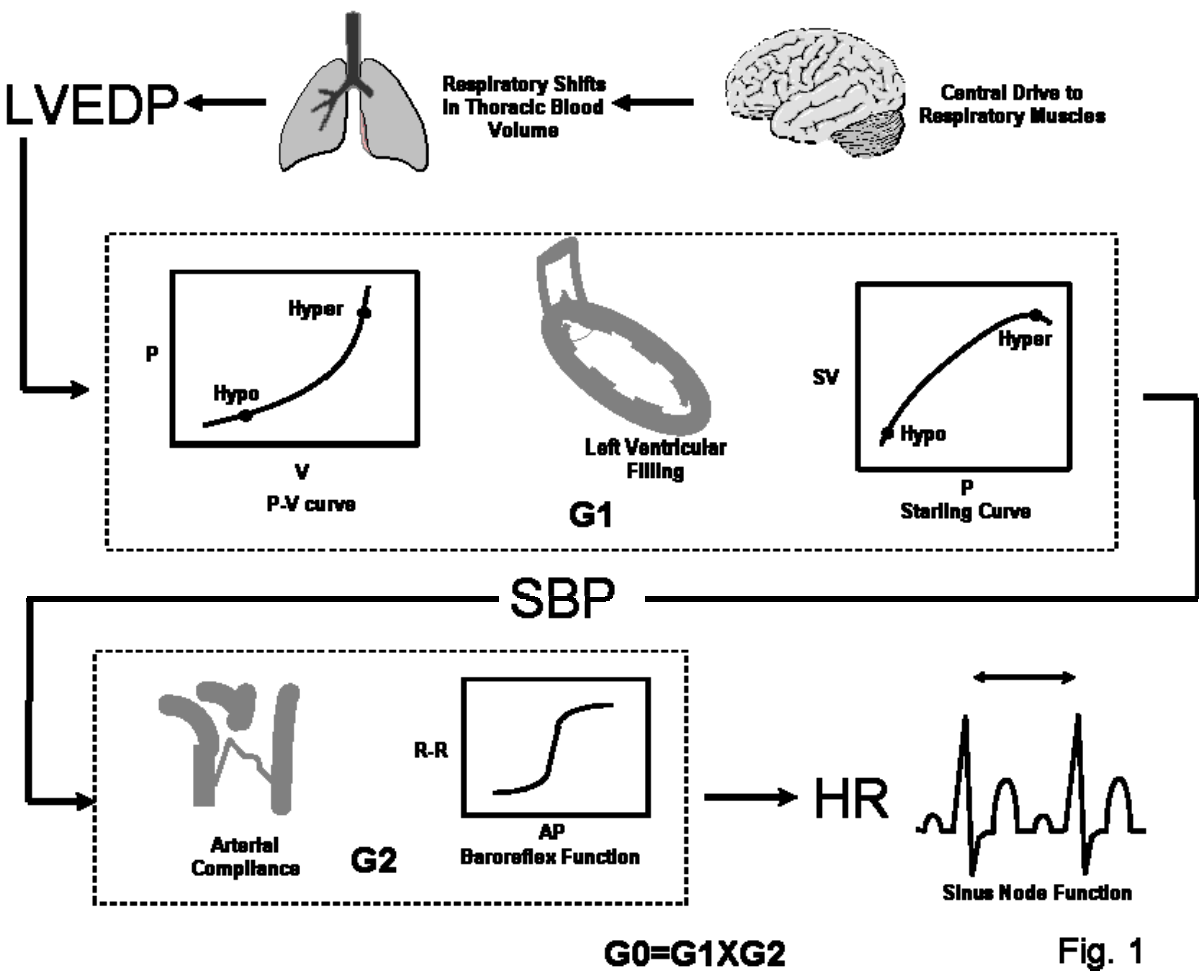


Fig. 1

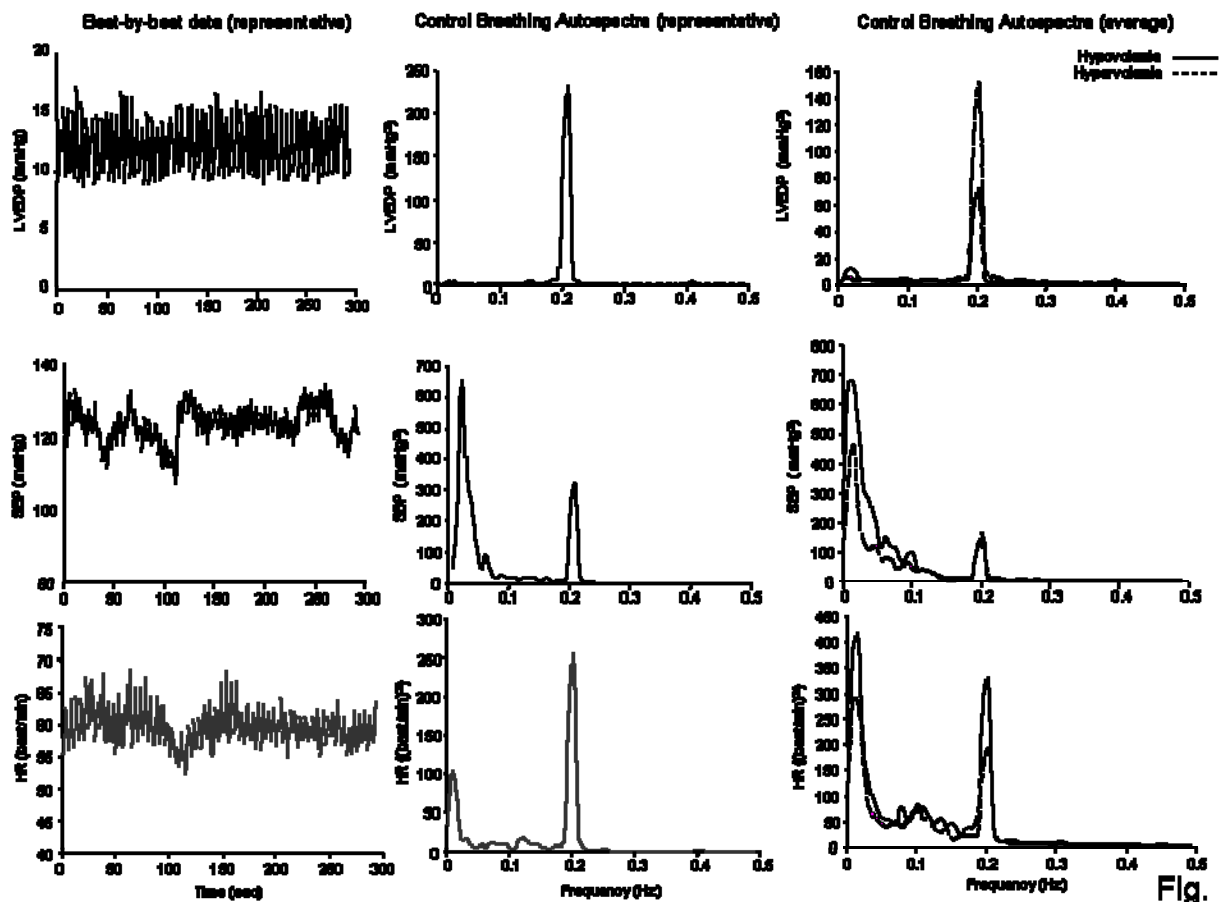


Fig. 2

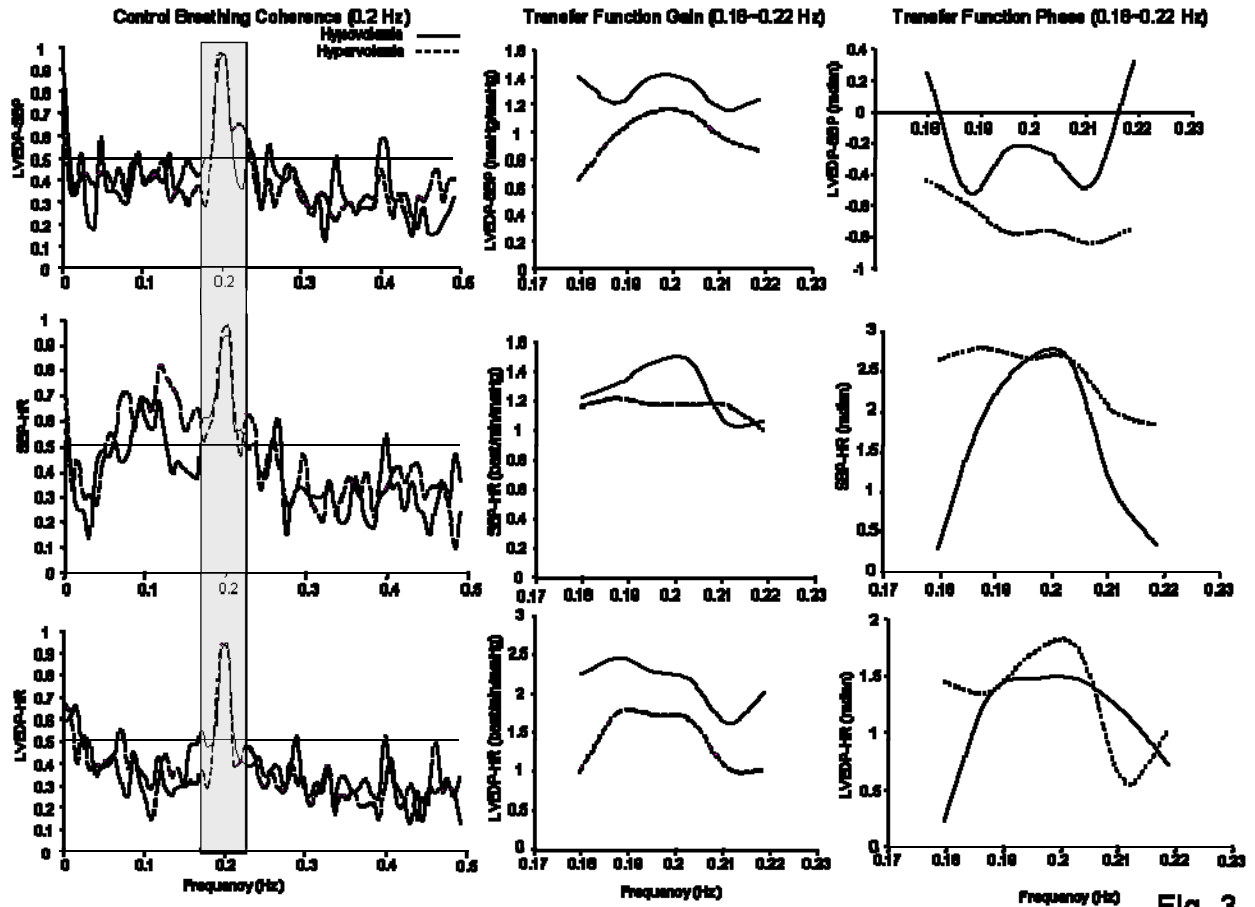


Fig. 3

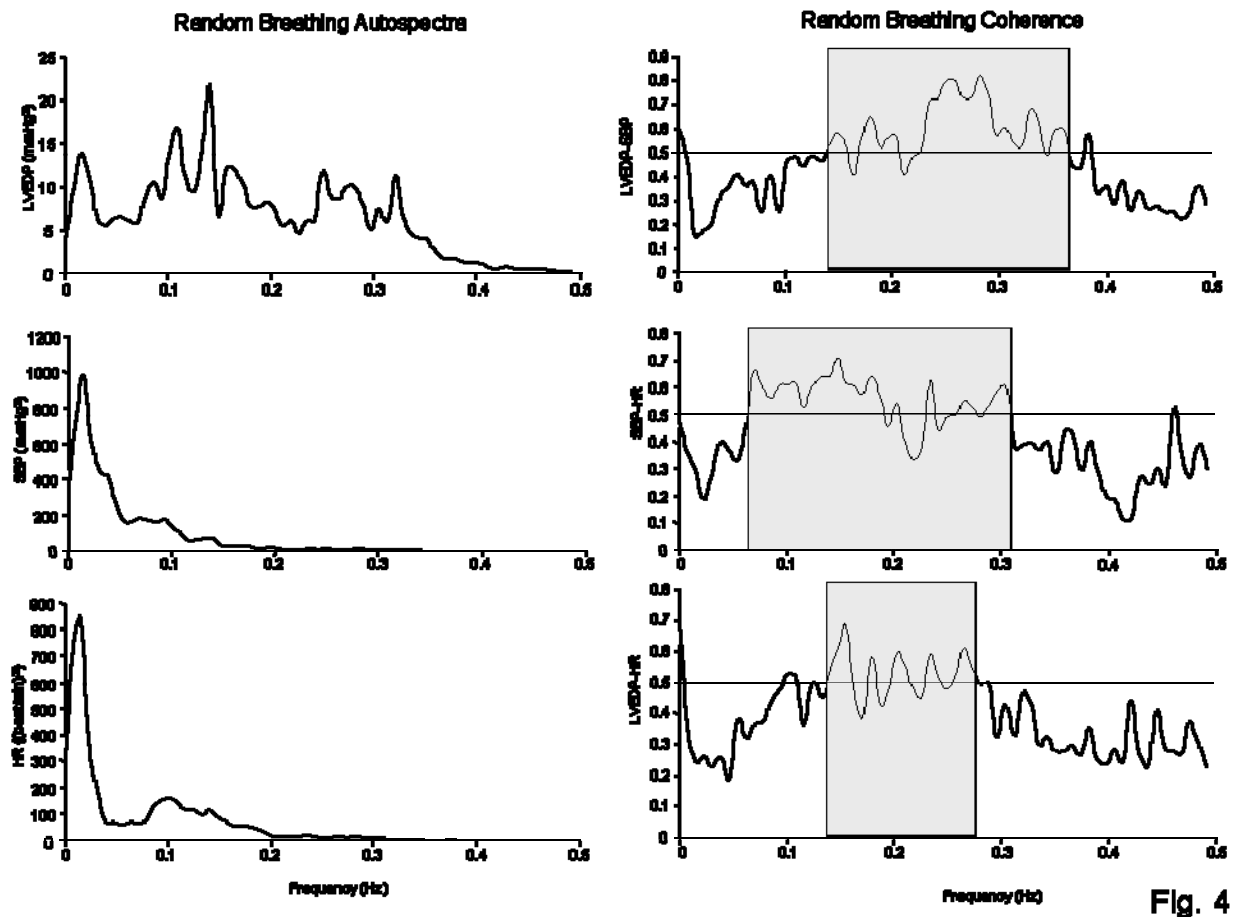
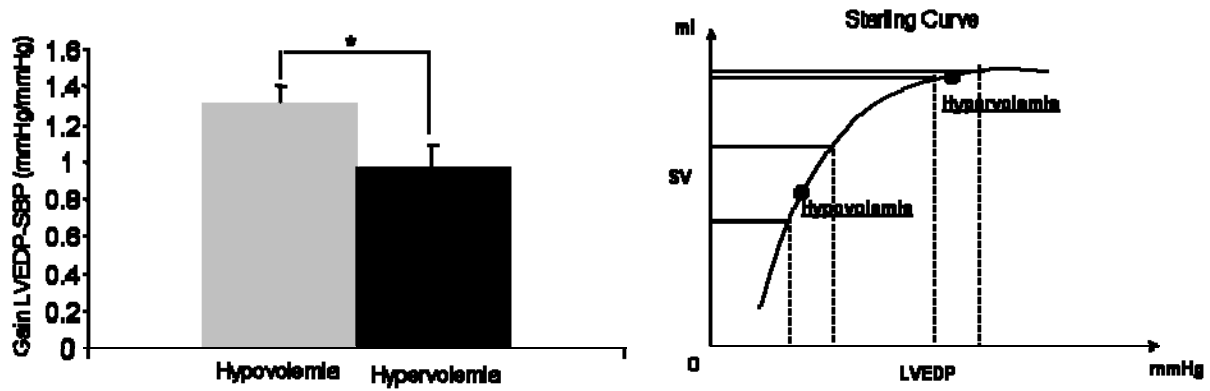
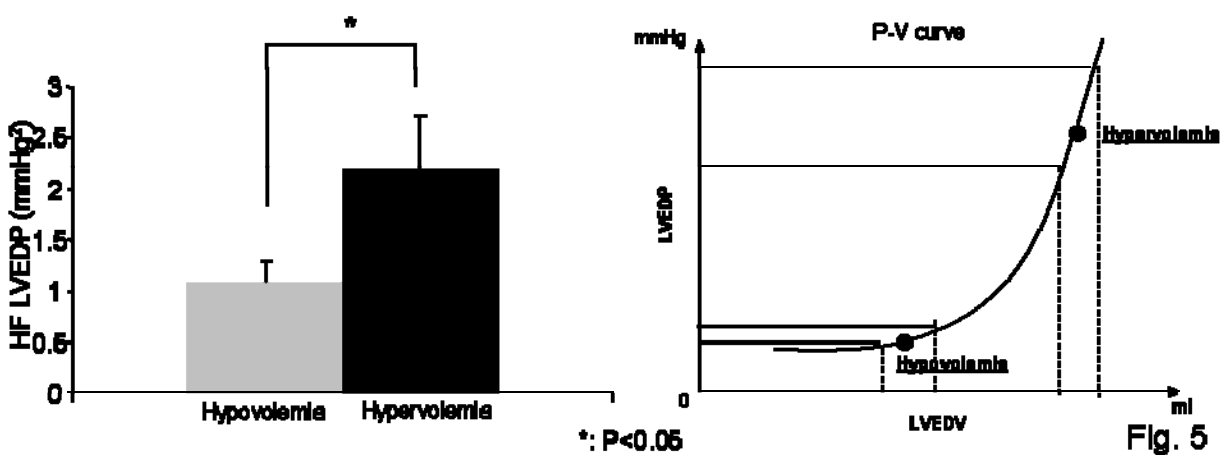


Fig. 4

Dynamic ventricular-arterial coupling Gain decreased in hypervolemia as expected from Starling Mechanisms



Respiratory changes in LVEDP increased in hypervolemia as expected from P-V relationship



\*: P<0.05

Fig. 5

## Reliability of cascade model

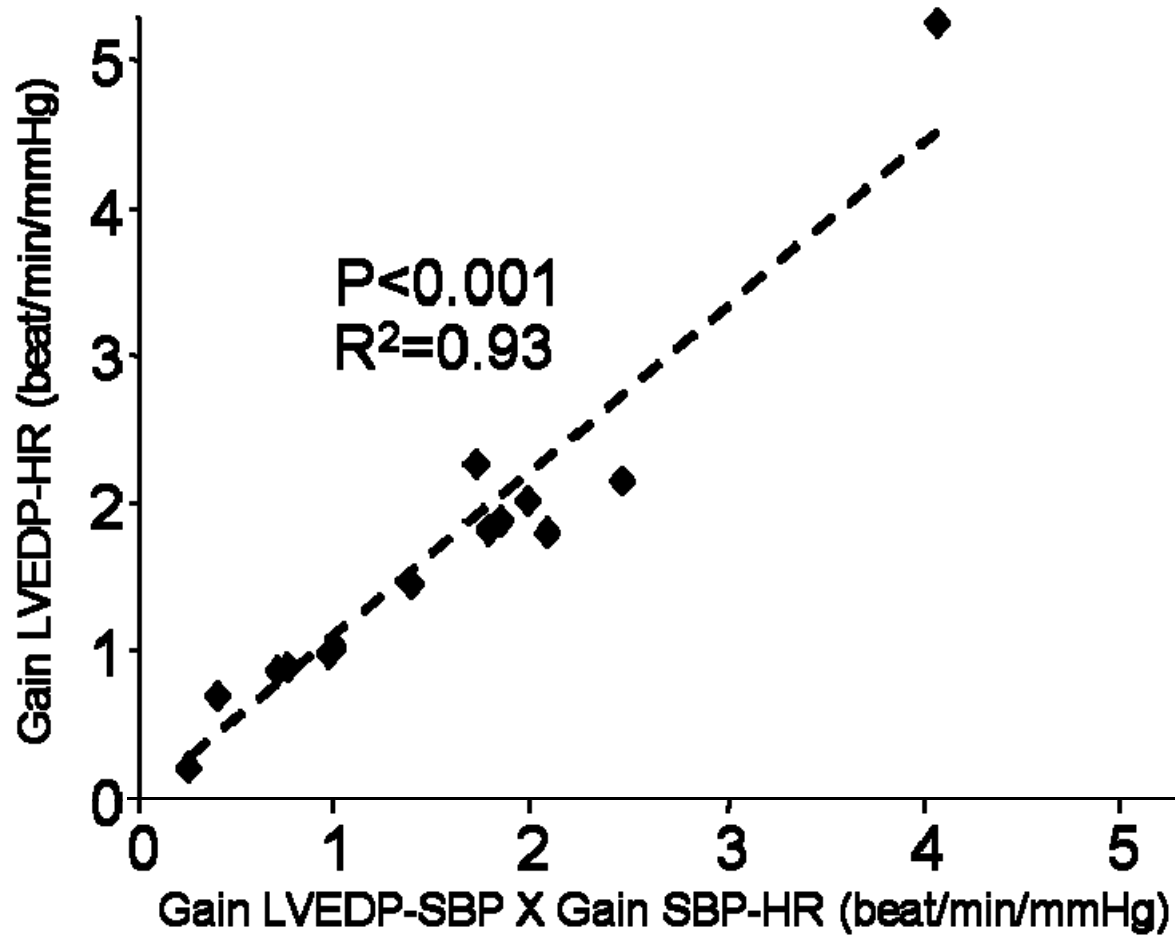
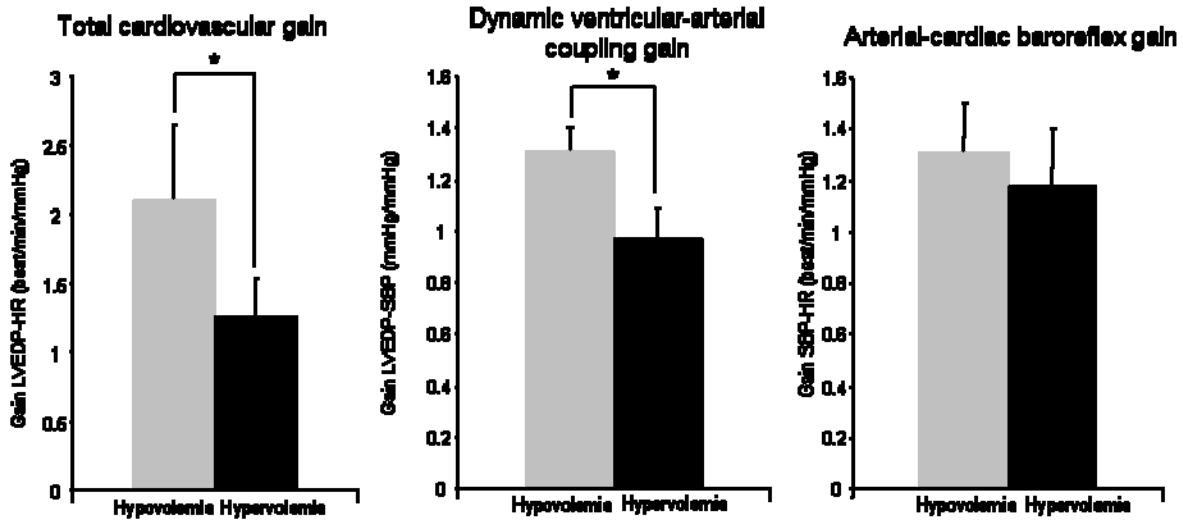
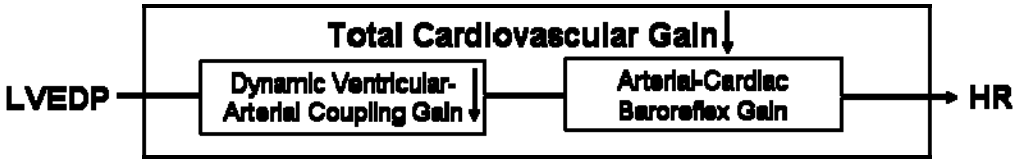


Fig. 6

**Total gain decreased in hypervolemia by the decreased dynamic ventricular-arterial coupling gain via cascade model**



\*: P<0.05 Fig. 7